



Supramolecular organization of α -galactosylceramide in pure dispersions and in cationic DODAB bilayers

Letícia S. Martins^a, Evandro L. Duarte^b, M. Teresa Lamy^b, Julio H.K. Rozenfeld^{a,*}

^a Departamento de Biofísica, Escola Paulista de Medicina, Universidade Federal de São Paulo, R. Botucatu 862, 04023-062, São Paulo, SP, Brazil

^b Instituto de Física, Universidade de São Paulo, Rua do Matão 1371, 05508090, São Paulo, SP, Brazil

ARTICLE INFO

Keywords:

α -galactosylceramide
glycosphingolipid
dioctadecyldimethylammonium bromide
cationic bilayers
differential scanning calorimetry
electron spin resonance spectroscopy

ABSTRACT

α -galactosylceramide (α -GalCer; KR7000) strongly stimulates NKT cells. The structures of α -GalCer assemblies and of cationic DODAB bilayers containing α -GalCer were investigated by differential scanning calorimetry (DSC) and electron spin resonance (ESR) spectroscopy. Assemblies of α -GalCer have a very tightly packed gel phase, causing spin labels to cluster and display spin exchange interactions. An endothermic phase transition is observed by DSC, leading to a fluid phase. This phase transition peak disappears upon mixing with DODAB, showing that up to 9 mol% α -GalCer is miscible with the cationic lipid. ESR spectra show that α -GalCer decreases DODAB gel phase packing, resulting in a decrease of gel-fluid transition temperature and cooperativity in DSC thermograms of mixed bilayers. In contrast, α -GalCer increases the rigidity of the fluid phase. These effects are probably due to the conformation of the rigid amide bond that connects the phytosphingosine base of α -GalCer to its long and saturated acyl chain. Possibly, α -GalCer adopts a V-shaped conformation because of the perpendicular orientation of the amide bond towards the axes of the hydrocarbon chains. Apparently, the effect of the amide bond configuration is a key structural feature for the interaction between ceramide-based glycolipids and DODAB molecules, since we have previously reported a similar decrease of gel phase packing and increase in fluid phase rigidity for DODAB bilayers containing C24:1 β -glucosylceramide. Since the structure of delivery systems is critical to the biological activity of α -GalCer, this work certainly contributes to the planning and development of novel immunotherapeutic tools.

1. Introduction

α -galactosylceramide (α -GalCer, also known as KR7000, Fig. 1) is a synthetic derivative of glycosphingolipids from the marine sponge *Agelas mauritanus*.¹ Its structure comprises a galactosyl residue α -linked to a ceramide (Fig. 1), and this ceramide corresponds to an 18-carbon phytosphingosine which is amide-linked to a 26-carbon saturated acyl chain.^{2,3}

This molecular structure enables α -GalCer presentation by Cluster of Differentiation 1 (CD1) molecules to Natural Killer T (NKT) cells, which become strongly activated.^{2,4,5} The activated NKT cells produce an array of cytokines that can stimulate the maturation of dendritic cells⁶, the activation of Natural Killer cells, B and CD8⁺ T lymphocytes^{7,8,9}, and even the conversion of myeloid-derived suppressor cells to immunogenic antigen presenting cells.¹⁰ In this case, α -GalCer significantly prolonged survival time in metastatic tumor-bearing mice.¹⁰ The broad and potent immunostimulatory effects of α -GalCer have been explored

in the treatment of cancer^{11,12,13} and in the development of vaccines.^{14,15,16}

In order to avoid toxicity¹⁷ and improve bioavailability, many delivery systems have been tested for α -GalCer, such as polymer nanoparticles^{18,19}, polymer micelles²⁰ and liposomes.^{21,22}

Dioctadecyldimethylammonium bromide (DODAB, Fig. 1) is a synthetic cationic lipid whose bilayers have been successfully employed as vaccine adjuvants.^{23,24} Hence, it could serve as a suitable carrier for α -GalCer. Indeed, DODAB bilayers containing TDB, a glycolipid derived from *Mycobacterium* cord factor, were shown to induce strong immune responses.²⁵

Physicochemical properties are very important in the design of bilayer-based immunotherapeutic tools: liposomes with greater bilayer rigidity and higher phase transition temperatures usually elicit higher antibody and cell-mediated immune responses.²⁶ Despite this importance, the structural properties of pure α -GalCer assemblies and their mixtures with other lipids are poorly characterized.

* Corresponding author.

E-mail address: julio.rozenfeld@unifesp.br (J.H.K. Rozenfeld).

Hence, in the present work, pure α -GalCer assemblies and DODAB bilayers prepared with different α -GalCer molar fractions were characterized by means of differential scanning calorimetry (DSC) and electron spin resonance (ESR) spectroscopy.

2. Materials and Methods

2.1. Materials

(2S,3S,4R)-1-O-(D-galactosyl)-N-hexacosanoyl-2-amino-1,3,4-octadecanetriol (α -GalCer) and the spin labels 1-palmitoyl-2-(*n*-doxylsearoyl)-*sn*-glycero-3-phosphocholine (*n*-PCSL, $n = 5$ or 16) were purchased from Avanti Polar Lipids (Birmingham, AL, USA). Dioctadecyldimethylammonium bromide (DODAB) and HEPES buffer were supplied by Sigma Chemical Co. (St. Louis, MO, USA). The chemical structures of α -GalCer, DODAB, 5- and 16-PCSL are shown in Fig. 1.

2.2. Membrane preparation

Chloroform/methanol 2:1 (v/v) solutions containing DODAB, α -GalCer or its mixtures, were dried under a stream of N_2 and left under reduced pressure for 2 h to form lipid films. Membranes were prepared by adding HEPES buffer (10 mM, pH 7.4) to the films and heating them for 15 min at 87 °C. Heating was accompanied by vigorous vortexing at every 5 minutes in order to ensure a homogenous dispersion. For ESR experiments, 0.8 mol% 5-PCSL or 0.3 mol% 16-PCSL were added to the chloroform/methanol solutions when preparing the lipid films. For DSC experiments, final lipid concentrations were 2 mM DODAB, 0.2 mM

α -GalCer or 2 mM DODAB plus 0.02 mM or 0.2 mM α -GalCer (which corresponds, respectively, to 0.9 mol% and 9 mol% of the total lipid concentration in the mixed membranes). For ESR experiments, final lipid concentrations were 2 mM DODAB, 2 mM α -GalCer or 2 mM DODAB plus 0.2 mM α -GalCer.

2.3. Differential Scanning Calorimetry (DSC)

DSC scans were performed in a PEAQ-DSC Microcalorimeter (Malvern Instruments Inc., Northampton, MA, USA). Heating rates were 20 °C/h. Scans were performed at least in duplicate. Thermograms correspond to second upscan.

2.4. ESR spectroscopy

ESR spectra at X-band (9.44 GHz) were obtained with a Bruker EMX spectrometer using a high sensitivity ER4119HS cavity. Microwave power was 13.4 mW, modulation frequency was 100 kHz and modulation amplitude was 1 G. The averaging number of scans was 20 for the temperature range of the gel phase and 5 for the temperature range of the fluid phase. All experiments were repeated at least once using different samples on different occasions. Empirical data correspond to the means of experiments with different samples, and standard deviations of these samples are shown as error bars.

The effective order parameter, S_{eff} , was calculated from the expression²⁷

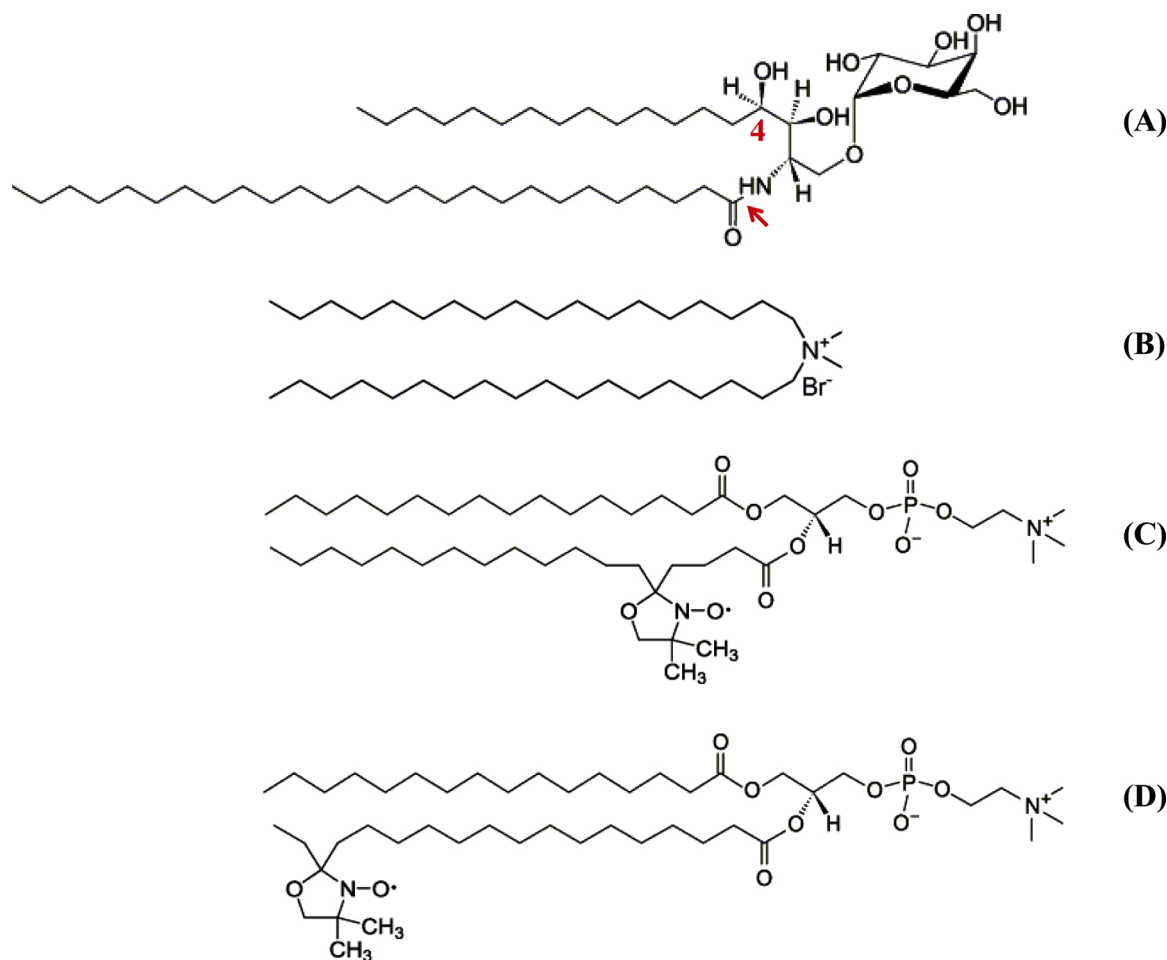


Fig. 1. Chemical structures of α -GalCer (A), DODAB (B), 5-PCSL (C) and 16-PCSL (D). In (A), the arrow indicates the amide bond connecting the acyl chain to the phytosphingosine and the number 4 indicates the hydroxyl group bonded to carbon 4 of the phytosphingosine.

$$S_{\text{eff}} = \frac{A_{\parallel} - A_{\perp}}{A_{zz} - (1/2)(A_{xx} + A_{yy})} \frac{a_o'}{a_o}$$

where $a_o' = (1/3)(A_{xx} + A_{yy} + A_{zz})$, $a_o = (1/3)(A_{\parallel} + 2A_{\perp})$, $A_{\parallel} (= A_{\text{max}})$ is the maximum hyperfine splitting directly measured in the spectrum (see Fig. 5), $A_{\perp} = A_{\text{min}} + 1.4 \left[1 - \frac{A_{\parallel} - A_{\text{min}}}{A_{zz} - (1/2)(A_{xx} + A_{yy})} \right]$, A_{min} is the measured inner hyperfine splitting (see Fig. 4) and A_{xx} , A_{yy} and A_{zz} are the principal values of the hyperfine tensor for doxylpropane.²⁸

The ratios between the low and central (h_{+1}/h_0) and the high and central field line amplitudes (h_{-1}/h_0) were also directly taken from spectra (see Figs. 3 and 5).

3. Results

3.1. The gel-fluid transition temperature and cooperativity of DODAB bilayers are decreased upon mixing with α -GalCer

The thermotropic behaviors of 2 mM DODAB, 0.2 mM α -GalCer and mixtures of 2 mM DODAB and α -GalCer are shown in Fig. 2.

DODAB bilayers prepared in HEPES buffer display a narrow transition beginning around 42 °C, peaking around 47 °C and ending around 49 °C, as previously observed.^{29,30}

Addition of α -GalCer shifts the transition to lower temperature and makes it broader: in presence of 0.02 mM α -GalCer, the transition begins around 35 °C, peaks around 46.6 °C and ends around 48.2 °C; in presence of 0.2 mM α -GalCer, the transition also begins around 35 °C, peaks around 44.3 °C and ends around 47.4 °C (Fig. 2). The broadening of the transition range indicates a decrease in cooperativity when α -GalCer is added to the DODAB bilayers.

Pure α -GalCer assemblies display a broad endothermic transition beginning around 64 °C, peaking at 72.5 °C and ending around 76.2 °C. A shoulder is also observed around 65.2 °C (Fig. 2). Similarly, a single endothermic peak at 72.8 °C has been described for α -GalCer prepared in 10 mM Tris-HCl, 150 mM NaCl, pH 7.0 and scanned at 60 °C/h.³¹

3.2. DODAB gel phase packing is decreased in mixtures with α -GalCer

Since 0.2 mM α -GalCer produced the strongest effect in the

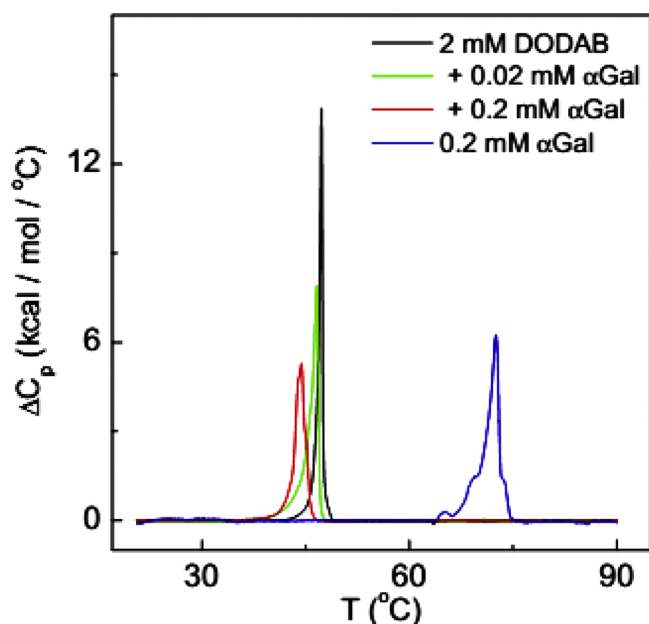


Fig. 2. Effect of α -GalCer on the DSC thermogram of 2 mM DODAB bilayers. Scan rate was 20 °C/h.

thermograms of mixed bilayers, ESR spectroscopy was used to compare the structures of pure 2 mM DODAB and mixed 2 mM DODAB + 0.2 mM α -GalCer bilayers. This technique uses phospholipids labelled with paramagnetic moieties at different positions to probe membrane structure at different depths, especially viscosity or packing.³² The spin label 5-PCSL, for example, gives information about the region closer to the water interface, whereas the spin label 16-PCSL informs about the bilayer core (Fig. 1). Spectra of 5- and 16-PCSL embedded in pure and mixed bilayers at temperatures below the DODAB gel-fluid phase transition are shown in Fig. 3.

In pure DODAB bilayers, the spectra of 5-PCSL are more anisotropic than the ones of 16-PCSL, showing that the former probe is in a more packed environment than the latter (Fig. 3). This flexibility gradient towards the membrane core is typical of the DODAB gel phase^{29,33} and



Fig. 3. Effect of 0.2 mM α -GalCer on ESR spectra of 5-PCSL and 16-PCSL embedded in 2 mM DODAB bilayers at temperatures below the gel-fluid transition. The maximum hyperfine splitting (A_{max}) and the amplitudes of low (h_{+1}) and central (h_0) fields are indicated. Total spectra width is 100 G.

is also observed in mixed bilayers of DODAB and α -GalCer. In fact, the spectra profiles of both probes are similar in pure and mixed bilayers (Fig. 3). Hence, empirical parameters obtained from the spectra can be more useful to compare these bilayers (Fig. 4).

The maximum hyperfine splitting (A_{max}) is an important parameter obtained from 5-PCSL spectra in the gel phase (Fig. 3). A_{max} values decrease as viscosity or packing decreases. It is important to have in mind that when we mention a decrease in viscosity or packing, it could be an increase in mobility and/or in bilayer disorder as it is not possible to distinguish between the two effects.³² As expected, Fig. 4A shows that A_{max} values decrease with increasing temperature in both types of bilayers. However, the lower A_{max} values for the DODAB+ α -GalCer bilayers indicate that they are less packed near the surface when compared to pure DODAB bilayers (Fig. 4A).

The spectra of 16-PCSL are more isotropic, and the A_{max} values cannot be accurately measured (Fig. 3). In this case, the ratio of the low and the central field line amplitudes (h_{+1}/h_0) provides better

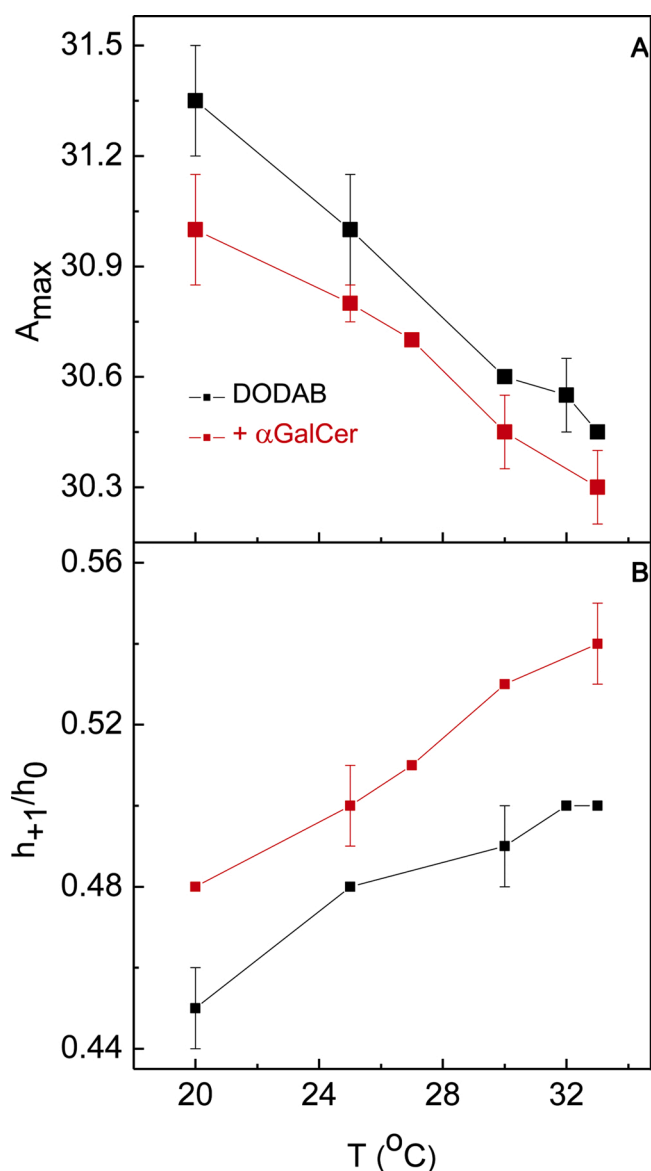


Fig. 4. Effect of 0.2 mM α -GalCer on the maximum hyperfine splitting (A_{max}) of 5-PCSL (A) and on the ratio of the low and the central field line amplitudes (h_{+1}/h_0) of 16-PCSL (B) embedded in 2 mM DODAB bilayers at the gel phase. Error bars indicate standard deviations of at least two experiments with different samples.

information on the bilayer structure, since its values increase as the bilayer becomes less packed.³² Accordingly, Fig. 4B shows that an increase in temperature and the resulting decrease in packing lead to an increase in h_{+1}/h_0 values. The higher h_{+1}/h_0 values for the mixed bilayers show that they are less packed at the core than the pure DODAB bilayers (Fig. 4B). In summary, the A_{max} and h_{+1}/h_0 values show that the DODAB+ α -GalCer bilayers are less tightly packed in the gel phase than the pure DODAB bilayers.

3.3. α -GalCer rigidifies the DODAB fluid phase

Spectra of 5- and 16-PCSL embedded in pure and mixed bilayers at



Fig. 5. Effect of 0.2 mM α -GalCer on ESR spectra of 5-PCSL and 16-PCSL embedded in 2 mM DODAB bilayers at temperatures above the gel-fluid transition. Maximum and minimum hyperfine splittings (A_{max} and A_{min}), and the amplitudes of central (h_0) and high (h_{-1}) field lines are indicated. Total spectra width is 100 G.

temperatures above the DODAB gel-fluid phase transition are shown in Fig. 5.

When compared to the spectra at lower temperatures (Fig. 3), the spectra of 5-PCSL display a profile with thinner features, where the A_{min} value can be clearly measured (Fig. 5). These features indicate that the probes have fast movement along their long axis²⁸ suggesting a fluid yet ordered location that is characteristic of a location close to the membrane interface in the fluid phase. The spectra of 5-PCSL in pure and mixed bilayers are similar (Fig. 5).

The sharp peaks observed in the spectra of 16-PCSL (Fig. 5) indicate a fast and nearly isotropic movement of the paramagnetic probe at the bilayer core, which is characteristic of the fluid phase.²⁸ No evident difference is observed in the spectra profiles of 16-PCSL embedded in pure DODAB or DODAB+ α -GalCer bilayers. Again, empirical parameters can be more informative on the structural differences between pure and mixed bilayers (Fig. 6).

The 5-PCSL spectra have clearly defined maximum and minimum hyperfine splittings (A_{max} and A_{min}) (Fig. 5), which can be used to

calculate an effective order parameter (S_{eff}), as described in Section 2.4. This parameter is useful to evaluate the acyl chain order, although it has been shown to have contributions from the paramagnetic label mobility.^{32,34,35} Fig. 6A shows that S_{eff} values are higher for mixed bilayers than for pure DODAB bilayers, indicating that the bilayer order close to the interface in the fluid phase is increased in the presence of α -GalCer.

The more isotropic spectra of 16-PCSL do not allow the measurements of the hyperfine splittings (Fig. 5). Hence, the ratio of the amplitude of the high and central field lines (h_{-1}/h_0), which are shown in Fig. 5, can be used to evaluate the membrane viscosity or packing.³² The h_{-1}/h_0 ratio increases as the bilayer viscosity decreases.³⁶ Indeed, Fig. 6B shows an increase of this ratio as the temperature increases and viscosity decreases as a result. The h_{-1}/h_0 ratio values are higher for pure DODAB bilayers than for mixed bilayers (Fig. 6B), indicating that α -GalCer rigidifies the core of DODAB bilayers in the fluid phase. In summary, an increase in rigidity is observed near the bilayer surface and at the bilayer core when α -GalCer is added to fluid DODAB bilayers.

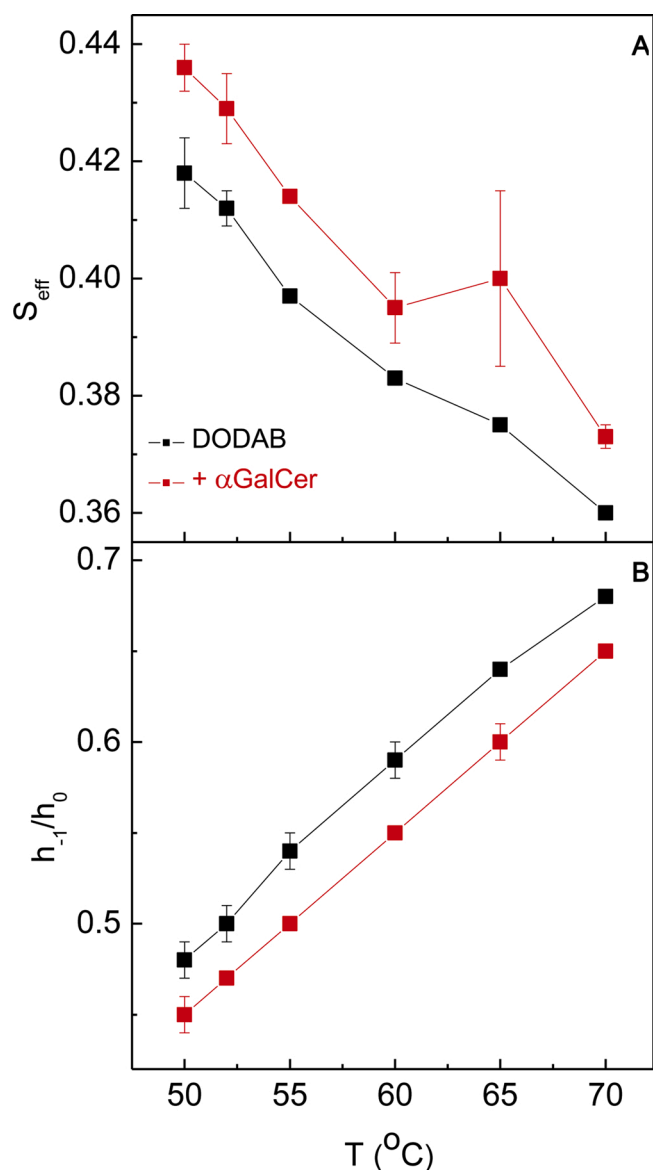


Fig. 6. Effect of 0.2 mM α -GalCer on the effective order parameter (S_{eff}) of 5-PCSL (A) and on the h_{-1}/h_0 ratios of 16-PCSL (B) embedded in 2 mM DODAB bilayers at the fluid phase. Error bars indicate standard deviations of at least two experiments with different samples.

3.4. Pure α -GalCer assemblies form thermotropic phases that interact differently with the spin labels

The ESR experiments with pure α -GalCer were performed with a

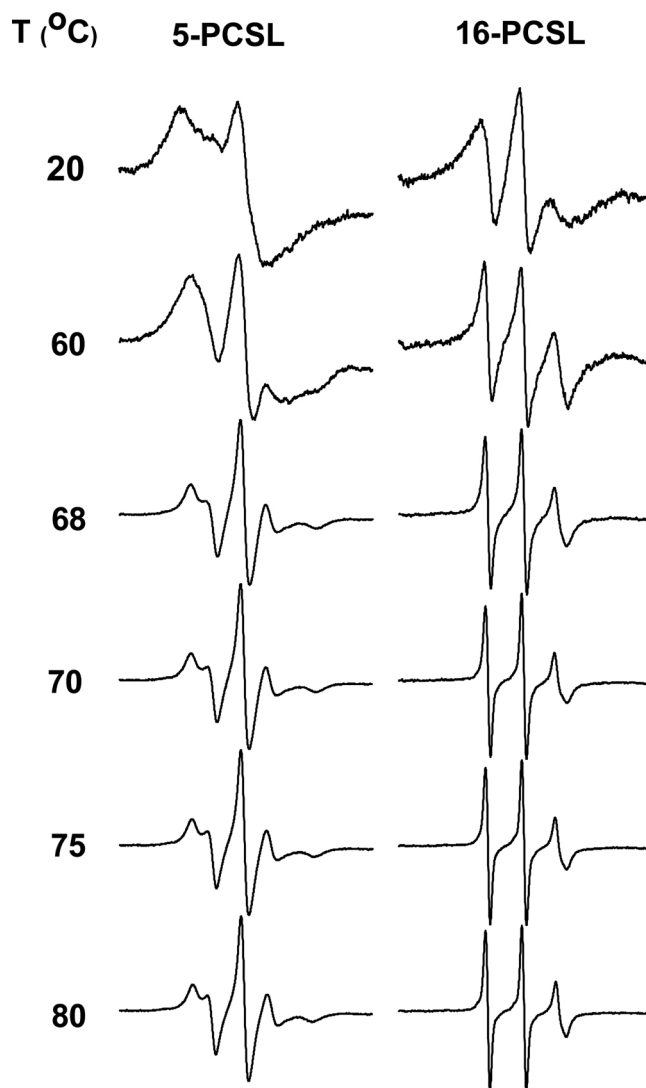


Fig. 7. Effect of temperature on the ESR spectra of 5-PCSL and 16-PCSL embedded in assemblies of 2 mM α -GalCer. Total spectra width is 100 G.

higher glycolipid concentration (2 mM) in order to improve the signal-to-noise ratio. Fig. 7 shows the ESR spectra of 5- and 16-PCSL in pure α -GalCer assemblies. It is important to note that pure 5- and 16-PCSL in aqueous solution do not display any measurable ESR signal, possibly due to low solubility. There must be some mixing with another lipid in order to observe an ESR spectrum with these paramagnetic probes.

At 20 °C and 60 °C, the spectra of both paramagnetic probes show broad and poorly defined peaks (Fig. 7), with a baseline typical of the presence of spin-spin exchange³⁷ which complicates the analysis of the ESR signals.

From 68 °C to 80 °C, the peaks in the spectra of 5- and 16-PCSL become more defined (Fig. 7). These ESR spectra indicate that the assemblies get more fluid as the temperature increases. It is also possible to observe that the spectra of 16-PCSL is more isotropic than the spectra of 5-PCSL (Fig. 7), suggesting that α -GalCer molecules are organized in bilayers, as a flexibility gradient from the polar heads to the end of the acyl chains is present in the more fluid phase.

4. Discussion

Hydration of α -GalCer films above 80 °C was shown to form dispersions with lamellar structure.³¹ These dispersions are organized in a gel phase below 72 °C, and extensive annealing at 37 °C could lead to further molecular packing without significantly changing the bilayer thickness³¹, probably by forming a subgel phase.

In the temperature range of 20 °C to 60 °C, spin-spin exchange interactions are obvious in the ESR spectra of 5- and 16-PCSL embedded in these lamellar α -GalCer dispersions (Fig. 7). Considering that very minute molar fractions of the probes were used, this suggests that they are forming clusters within the α -GalCer assemblies at these temperatures.

It was shown that α -GalCer monolayers at 20 °C and 37 °C form a very tightly packed condensed phase with no rotational freedom, possibly due to strong and rigid intermolecular hydrogen bonds between the galactosyl headgroups.³⁸ Such ordered and packed organization of α -GalCer molecules could explain the formation of spin label clusters and the resulting spin-spin interactions at low temperatures.

In contrast, ESR spectra of 5- and 16-PCSL at the same 20 °C to 60 °C temperature range do not show spin-spin interactions in pure C24:1 β -glucosylceramide dispersions.²⁹ C24:1 β -glucosylceramide has an unsaturated acyl chain and a more hydrated glucosyl headgroup³⁹ that could hinder tight chain packing and strong headgroup interactions as observed for α -GalCer.³⁸ Moreover, the hydroxyl group in position 4 of the α -GalCer sphingoid base (Fig. 1) might participate in the hydrogen bonding network. This hydroxyl is replaced by a *trans* double bond in C24:1 β -glucosylceramide.²⁹

Above 68 °C, the ESR spectra in pure α -GalCer assemblies are typical of a lamellar fluid phase (Fig. 7). In fact, the spectra profiles of both probes are similar to the ones observed for mixed DODAB+ α -GalCer bilayers in the fluid phase (Fig. 5).

The spectra profiles of both probes in pure α -GalCer assemblies change significantly from 60 °C to 68 °C (Fig. 7). These changes are consistent with the broad phase transition beginning at 64 °C that is observed in the thermogram of pure α -GalCer (Fig. 2).

The α -GalCer thermogram has an endothermic peak in 72.5 °C (Fig. 2), but very isotropic spectra characteristic of a fluid phase are already observed at 70 °C (Fig. 7). This difference in the phase transition temperature range might be due to the different concentrations tested in the DSC and the ESR assays (Figs. 2 and 7). Similarly, the phase transition temperature range was different when ESR spectra from 2 mM samples were compared to the thermogram of 0.2 mM C24:1 β -glucosylceramide.²⁹ It is also interesting to note that α -GalCer and its analog containing an alkyl amino linker at the C6 hydroxy group of galactose displayed the same structural properties but very different thermodynamic properties.³⁸ This highlights the need of different techniques to investigate the organization of supramolecular assemblies.

The α -GalCer endothermic peak at 72.5 °C completely disappears in mixed bilayers (Fig. 2), suggesting that up to 9 mol% of α -GalCer is miscible with DODAB. Similarly, α -GalCer was shown to be miscible in DPPC bilayers up to 30 mol%.³¹ Increasing the α -GalCer molar fractions in mixed bilayers resulted in broader transitions shifted to lower temperatures (Fig. 2), indicating that α -GalCer decreases the transition temperature and the cooperativity of DODAB bilayers.

The large mismatch between the acyl chain of α -GalCer and DODAB (Fig. 1) would permit transbilayer interdigitation and an increased coupling of structural and dynamic properties of the two lamellar monolayers.⁴⁰ As a result, it would be expected an increase in phase transition temperature of DODAB+ α -GalCer bilayers when compared to pure DODAB bilayers, as seen in mixtures of galactosylceramide and dimyristoylphosphatidylcholine.⁴¹

X-ray scattering of pure α -GalCer bilayers show a small lamellar periodicity, possibly resulting from an interdigitated and tilted organization of the hydrocarbon chains.³¹ If that was the case for α -GalCer in mixed bilayers in the gel phase, it would be expected that the 16-PCSL probe would sense a more motionally restricted and/or ordered environment than in pure DODAB bilayers.⁴² That is clearly not the case, since the h_{+1}/h_0 values are higher for mixed than for pure bilayers (Fig. 4B), i.e., the DODAB+ α -GalCer bilayers are less packed at the core than the pure DODAB bilayers. Moreover, A_{max} values are smaller for 5-PCSL in mixed bilayers, indicating that these bilayers are also less packed near the surface (Fig. 4A). This decrease in the gel phase packing is consistent with the decrease in cooperativity and phase transition temperature observed in thermograms of DODAB+ α -GalCer bilayers (Fig. 2).

A possible explanation for the absence of gel phase interdigitation despite the large chain mismatch of the mixed lipids resides in the amide bond that connects the acyl chain to the phytosphingosine base of α -GalCer (Fig. 1). This bond is known to adopt a rigid resonance structure comprising six atoms organized in a planar *trans* configuration.⁴³ In ceramides, the amide bond adopts a perpendicular orientation towards the axes of the two hydrocarbon chains.⁴⁴ Single crystal analyses of tetracosanoylphytosphingosine, which has a saturated 24-carbon acyl chain, show that this configuration of the amide bond results in a V-shaped molecular conformation.⁴⁴ Similarly, it was shown for phospholipids that a kink near the headgroup would allow a rotation of the rest of the chain with no associated local flexing.⁴⁵

α -GalCer could also adopt this V-shaped conformation, and the bulky and hydrated galactosyl group could further stabilize it (Fig. 1). In that case, the large lateral area requirement would result in increased hydrophobic defects and decreased packing of the DODAB gel phase, consistent with the ESR spectra results (Figs. 3 and 4).

The V-shaped configuration could also explain the increase in DODAB fluid phase rigidity induced by α -GalCer (Fig. 6). The smaller h_{+1}/h_0 ratio values of 16-PCSL for mixed bilayers show that α -GalCer increases the membrane core viscosity (Fig. 6B). This increase in viscosity possibly results from a more limited motion of DODAB acyl chains. Similarly, α -GalCer increases the superficial bilayer order of the DODAB fluid phase, since the effective order parameter S_{eff} values are higher for the mixed bilayers (Fig. 6A). Considering that S_{eff} is strongly dependent on acyl chains segmental motion³⁵, the increase in surface bilayer order reflects the limited amplitude of acyl chains segmental motion caused by the expanded lateral area occupied by α -GalCer acyl chains. The rigidifying effect of α -GalCer could be further enhanced by the increased hydration of the galactosyl headgroup in the fluid phase. It was shown that the number of water molecules associated with glycolipid headgroups double upon transition to the fluid phase.⁴⁶ It is of note that spin-labeled galactosylceramides also induced an increase in rigidity of fluid phase membranes.⁴⁷

A similar decrease in transition temperature, cooperativity and gel phase packing plus an increase in fluid phase rigidity was observed in mixtures of DODAB and C24:1 β -glucosylceramide.²⁹ This glycolipid also has a long acyl chain, but has a *cis*-double bond that causes a kink in the

middle of the chain, and it lacks the hydroxyl group in position 4 of the α -GalCer sphingoid base, as pointed previously. Despite all this molecular differences, it also has an amide bond connecting the acyl chain to the sphingoid base. Hence, the amide bond configuration seems to be a key structural feature for the interaction between ceramide-based glycolipids and DODAB molecules.

Although pure α -GalCer dispersions can be formed by heating above 80 °C, i.e. above the phase transition temperature, much effort has been dedicated to develop carriers that are able to deliver this glycolipid to specific antigen presenting cells.⁴⁸ Another issue is the intracellular fate: efficient α -GalCer presentation by antigen presenting cells depends on the action of proteins called saposins, which are produced by proteolytic cleavage in the endosome.^{49,50} It was shown that fluid liposomes that direct α -GalCer to the endosomes and remain there enhance the glycolipid presentation by dendritic cells.⁵¹ Considering that DODAB is able to promote antigen capture and presentation by antigen presenting cells in an endocytic-dependent way⁵², and that α -GalCer fluidizes the DODAB membrane (Figs. 2 and 4), it is possible to suppose that DODAB bilayers would be suitable carriers for α -GalCer. As a next step, it would be interesting to compare the immunological effects of pure α -GalCer dispersions and mixed DODAB+ α -GalCer bilayers.

5. Conclusions

The structures of α -GalCer assemblies and of cationic DODAB bilayers containing α -GalCer were investigated by means of DSC and ESR spectroscopy. Pure α -GalCer assemblies were formed by hydration of lipid films above 80 °C. These assemblies have a very tightly packed gel phase up to 60 °C, causing spin labels to cluster and display spin-spin exchange interactions. An endothermic phase transition peaking at 72.5 °C is observed by DSC, leading to a fluid phase. This phase transition peak disappears upon mixing with DODAB, showing that up to 9 mol% α -GalCer is miscible within the DODAB bilayer.

Empirical data from ESR spectra show that α -GalCer decreases DODAB gel phase packing, resulting in a decrease of gel-fluid transition temperature and cooperativity in DSC thermograms of mixed bilayers. On the other hand, α -GalCer induced an increase in DODAB fluid phase rigidity. These effects are probably due to the conformation of the rigid amide bond that connects the phytosphingosine base of α -GalCer to its long and saturated acyl chain. Possibly, α -GalCer adopts a V-shaped conformation because of the perpendicular orientation of the amide bond towards the axes of the two hydrocarbon chains. Apparently, the structural effects of the amide bond configuration are a key structural feature for the interaction between ceramide-based glycolipids and DODAB molecules, since we have previously reported a similar decrease of gel phase packing and increase in fluid phase rigidity for DODAB bilayers containing C24:1 β -glucosylceramide.

Considering that the structure of delivery systems is critical to the biological activity of α -GalCer, the present work certainly contributes to the planning and development of new immunotherapeutic tools.

Acknowledgments

This work was supported by grants #2016/19077-1 and #2016/13368-4, São Paulo Research Foundation (FAPESP). This study was financed in part by the Coordenação de Aperfeiçoamento de Pessoal de Nível Superior - Brasil (CAPES) - Finance Code 001. L.S.M. is funded by a CAPES PhD fellowship and M.T.L. is recipient of a CNPq research fellowship. M.T.L. and E.L.D. are part of the National Institute of Science and Technology Complex Fluids (INCT-FCx), financed by CNPq (465259/2014-6) and FAPESP (2014/50983-3).

References

- [1] Birkholz, A.M., Howell, A.R., Kronenberg, M., 2015. The alpha and omega of galactosylceramides in T cell immune function. *J. Biol. Chem.* 290, 15365–15370.

- [2] Tsuji, M., 2006. Glycolipids and phospholipids as natural CD1d-binding NKT cell ligands. *Cell. Mol. Life Sci.* 63, 1889–1898.
- [3] Alititi, A.S., Ma, X., Zhang, L., Ban, Y., Franck, R.W., Mootoo, D.R., 2017. Synthesis and biological activities of C-glycosides of KRN 7000 with novel ceramide residues. *Carbohydr. Res.* 443–444, 73–77.
- [4] Burdin, N., Brossay, L., Koezuka, Y., Smiley, S.T., Grusby, M.J., Gui, M., Taniguchi, M., Hayakawa, K., Kronenberg, M., 1998. Selective ability of mouse CD1 to present glycolipids: alpha-galactosylceramide specifically stimulates V alpha 14⁺ NK T lymphocytes. *J. Immunol.* 161, 3271–3281.
- [5] Tyznik, A.J., Farber, E., Girardi, E., Birkholz, A., Li, Y., Chitale, S., So, R., Arora, P., Khurana, A., Wang, J., Porcelli, S.A., Zajonc, D., Kronenberg, M., Howell, A.R., 2011. Glycolipids that elicit IFN- γ -biased responses from natural killer T cells. *Chem. Biol.* 18, 1620–1630.
- [6] Fujii, S.I., Shimizu, K., Hemmi, H., Steinman, R.M., 2007. Innate V α 14⁺ natural killer T cells mature dendritic cells, leading to strong adaptive immunity. *Immunol. Rev.* 220, 183–198.
- [7] Metelitsa, L.S., Naidenko, O.V., Kant, A., Wu, H.W., Loza, M.J., Perussia, B., Kronenberg, M., Seeger, R.C., 2001. Human NKT cells mediate antitumor cytotoxicity directly by recognizing target cell CD1d with bound ligand or indirectly by producing IL-2 to activate NK cells. *J. Immunol.* 167, 3114–3122.
- [8] Galli, G., Nuti, S., Tavarini, S., Galli-Stampino, L., De Lalla, C., Casorati, G., Dellabona, P., Abrignani, S., 2003. CD1d-restricted help to B cells by human invariant natural killer T lymphocytes. *J. Exp. Med.* 197, 1051–1057.
- [9] Stober, D., Jomantaite, I., Schirmbeck, R., Reimann, J., 2003. NKT cells provide help for dendritic cell-dependent priming of MHC class I-restricted CD8⁺ T cells in vivo. *J. Immunol.* 170, 2540–2548.
- [10] Ko, H.J., Lee, J.M., Kim, Y.J., Kim, Y.S., Lee, K.A., Kang, C.Y., 2009. Immunosuppressive Myeloid-Derived Suppressor Cells can be converted into immunogenic APCs with the help of activated NKT cells: an alternative cell-based antitumor vaccine". *J. Immunol.* 182, 1818–1828.
- [11] Kobayashi, E., Motoki, K., Uchida, T., Fukushima, H., Koezuka, Y., 1995. KRN7000, a novel immunomodulator, and its antitumor activities. *Oncol. Res.* 7, 529–553.
- [12] Schneiders, F.L., Scheper, R.J., von Blomberg, B.M., Woltman, A.M., Janssen, H.L., van den Eertwegh, A.J., Verheul, H.M., de Groot, T.D., van der Vliet, H.J., 2011. Clinical experience with alpha-galactosylceramide (KRN7000) in patients with advanced cancer and chronic hepatitis B/C infection. *Clin. Immunol.* 140, 130–141.
- [13] King, L.A., Lameris, R., de Groot, T.D., van der Vliet, H.J., 2018. CD1d-invariant Natural Killer T cell-based cancer immunotherapy: α -galactosylceramide and beyond. *Front. Immunol.* 9, 1519.
- [14] Guillonnet, C., Mintern, J.D., Hubert, F.X., Hurt, A.C., Besra, G.S., Porcelli, S., Barr, I.G., Doherty, P.C., Godfrey, D.I., Turner, S.J., 2009. Combined NKT cell activation and influenza virus vaccination boosts memory CTL generation and protective immunity. *Proc. Natl. Acad. Sci. USA* 106, 3330–3335.
- [15] Carreño, L.J., Kharkwal, S.S., Porcelli, S.A., 2014. Optimizing NKT cell ligands as vaccine adjuvants. *Immunotherapy* 6, 309–320.
- [16] Bonam, S.R., Partidos, C.D., Halmuthur, S.K.M., Muller, S., 2017. An overview of novel adjuvants designed for improving vaccine efficacy. *Trends Pharmacol. Sci.* 38, 771–793.
- [17] Osman, Y., Kawamura, T., Naito, T., Takeda, K., van Kaer, L., Okumura, K., Abo, T., 2000. Activation of hepatic NKT cells and subsequent liver injury following administration of α -galactosylceramide. *Eur. J. Immunol.* 30, 1919–192.
- [18] Macho-Fernandez, E., Cruz, L.J., Ghinnagow, R., Fontaine, J., Bialecki, E., Frisch, B., Trottein, F., Faveeuw, C., 2014. Targeted delivery of α -galactosylceramide to CD8 α ⁺ dendritic cells optimizes type I NKT cell-based antitumor responses. *J. Immunol.* 193, 961–969.
- [19] Gonzatti, M.B., Sousa, M.E.P., Tunissi, A.S., Mortara, R.A., Oliveira, A.M., Cerize, M.N.P., Keller, A.C., 2019. Nano spray dryer for vectorizing α -galactosylceramide in polymeric nanoparticles: a single step process to enhance invariant Natural Killer T lymphocyte responses. *Int. J. Pharm.* 565, 123–132.
- [20] Giaccone, G., Punt, C.J.A., Ando, Y., Ruijter, R., Nishi, N., Peters, M., von Blomberg, B.M.E., Scheper, R.J., van der Vliet, H.J.J., van den Eertwegh, A.J.M., Roelink, M., Beijnen, J., Zwierzina, H., Pinedo, H.M., 2002. A phase I study of the Natural Killer T-cell ligand α -galactosylceramide (KRN7000) in patients with solid tumors. *Clin. Canc. Res.* 8, 3702–3709.
- [21] Macho-Fernandez, E., Chekkat, N., Ehret, C., Thomann, J.S., De Giorgi, M., Spanedda, M.V., Bourel-Bonnet, L., Betbeder, D., Heurtault, B., Faveeuw, C., Fournel, S., Frisch, B., Trottein, F., 2017. Solubilization of α -galactosylceramide in aqueous medium: impact on Natural Killer T cell activation and antitumor responses. *Int. J. Pharm.* 530, 354–363.
- [22] Suzuki, S., Sakurai, D., Sakurai, T., Yonekura, S., Iinuma, T., Okuma, Y., Ihara, F., Arai, T., Hanazawa, T., Fukuda-Kawaguchi, E., Ishii, Y., Okamoto, Y., 2019. Sublingual administration of liposomes enclosing α -galactosylceramide as an effective adjuvant of allergen immunotherapy in a murine model of allergic rhinitis. *Allergol. Int.* 68, 352–362.
- [23] Rozenfeld, J.H.K., Silva, S.R., Ranéia, P.A., Faquim-Mauro, E., Carmona-Ribeiro, A.M., 2012. Stable assemblies of cationic bilayer fragments and CpG oligonucleotide with enhanced immunoadjuvant activity in vivo. *J. Contr. Release* 160, 367–373.
- [24] Aps, L.R.M.M., Tavares, M.B., Rozenfeld, J.H.K., Lamy, M.T., Ferreira, L.C.S.F., Diniz, M.O., 2016. Bacterial spores as particulate carriers for gene gun delivery of plasmid DNA. *J. Biotechnol.* 228, 58–66.
- [25] Davidsen, J., Rosenkrands, I., Christensen, D., Vangala, A., Kirby, D., Perrie, Y., Agger, E.M., Andersen, P., 2005. Characterization of cationic liposomes based on dimethyloctadecylammonium and synthetic cord factor from *M. tuberculosis* (trehalose 6,6'-dibehenate) - A novel adjuvant inducing both strong CMI and antibody responses. *Biochim. Biophys. Acta - Biomembr.* 1718, 22–31.

- [26] Watson, D.S., Endsley, A.N., Huang, L., 2012. Design considerations for liposomal vaccines: influence of formulation parameters on antibody and cell-mediated immune responses to liposome associated antigens. *Vaccine* 30, 2256–2272.
- [27] Boggs, J.M., Rangaraj, G., 1985. Phase transitions and fatty acid spin label behavior in interdigitated lipid phases induced by glycerol and polymixin. *Biochim. Biophys. Acta* 816, 221–233.
- [28] Hubbel, W.L., McConnell, H.M., 1971. Molecular motion in spin-labeled phospholipids and membranes. *J. Am. Chem. Soc.* 93, 314–326.
- [29] Martins, L.S., Nomura, D.A., Duarte, E.L., Riske, K.A., Lamy, M.T., Rozenfeld, J.H.K., 2019. Structural characterization of cationic DODAB bilayers containing C24:1 β -glucosylceramide. *Biochim. Biophys. Acta* 1861, 643–650.
- [30] Linseisen, F.M., Bayerl, S., Bayerl, T.M., 1996. 2H-NMR and DSC study of DPPC-DODAB mixtures. *Chem. Phys. Lipids* 83, 9–23.
- [31] Nakano, M., Inoue, R., Koda, M., Baba, T., Matsunaga, H., Natori, T., Handa, T., 2000. Anomeric effects on the stability of bilayers of galactosylphytoceramides and on the interaction with phospholipids. *Langmuir* 16, 7156–7161.
- [32] Rozenfeld, J.H.K., Duarte, E.L., Oliveira, T.R., Lamy, M.T., 2017. Structural insights on biologically relevant cationic membranes by ESR spectroscopy. *Biophys. Rev.* 9, 633–647.
- [33] Rozenfeld, J.H.K., Duarte, E.L., Barbosa, L.R.S., Lamy, M.T., 2015. The effect of an oligonucleotide on the structure of cationic DODAB vesicles. *Phys. Chem. Chem. Phys.* 17, 7498–7506.
- [34] Lange, A., Marsh, D., Wassmer, K.H., Meier, P., Kothe, G., 1985. Electron spin resonance study of phospholipid membranes employing a comprehensive line-shape model. *Biochemistry* 24, 4383–4392.
- [35] Schindler, H., Seelig, J., 1973. EPR spectra of spin labels in lipid bilayers. *J. Chem. Phys.* 59, 1841–1850.
- [36] Marsh, D., 1989. In: Berliner, L.J., Reuben, J. (Eds.), *Spin labeling. Theory and applications*, vol. 8. Plenum Press, New York, pp. 255–303.
- [37] Devaux, P., McConnell, H.M., 1972. Lateral Diffusion in Spin-Labeled Phosphatidylcholine Multilayers. *J. Am. Chem. Soc.* 94, 4475–4481.
- [38] Brezesinski, G., Calow, A.D.J., Pereira, C.L., Seeberger, P.H., 2020. Thermodynamic and structural behavior of α -galactosylceramide and C6-functionalized α -GalCer in 2D layers at the air-liquide interface. *ChemBioChem* 21, 241–247.
- [39] Róg, T., Vattulainen, I., Bunker, A., Karttunen, M., 2007. Glycolipid membranes through atomistic simulations: effect of glucose and galactose head groups on lipid bilayer properties. *J. Phys. Chem. B* 111, 10146–10154.
- [40] Dahlén, B., Pascher, I., 1979. Molecular arrangements in sphingolipids. Thermotropic phase behaviour of tetracosanoylphosphosphingosine. *Chem. Phys. Lipids* 24, 119–133.
- [41] Linington, C., Rumsby, M.G., 1981. Galactosyl ceramides of the myelin sheath: thermal studies. *Neurochem. Int.* 3, 211–218.
- [42] Boggs, J.M., Rangaraj, G., Watts, A., 1989. Behavior of spin labels in a variety of interdigitated lipid bilayers. *Biochim. Biophys. Acta* 981, 243–253.
- [43] Marsh, R.E., Donohue, J., 1967. Crystal structure studies of amino acids and proteins. *Adv. Protein Chem.* 22, 235–256.
- [44] Pascher, I., 1976. Molecular arrangements in sphingolipids Conformation and hydrogen bonding of ceramide and their implication on membrane stability and permeability. *Biochim. Biophys. Acta* 455, 433–451.
- [45] Seiter, C.H.A., Chan, S.I., 1973. Molecular motion in lipid bilayers. A nuclear magnetic resonance line width study. *J. Am. Chem. Soc.* 95, 7541–7553.
- [46] Köberl, M., Hinz, H.J., Rapp, G., 1998. Temperature scanning simultaneous small- and wide-angle X-ray scattering studies of glycolipid vesicles: areas, expansion coefficients and hydration. *Chem. Phys. Lipids* 91, 13–37.
- [47] Sharom, F.J., Grant, C.W.M., 1977. Glycosphingolipids in membrane architecture. *Journal of Supramolecular Structure* 6, 249–258.
- [48] Ghinnagow, R., Cruz, L.J., Macho-Fernandez, E., Faveeuw, C., Trottein, F., 2017. Enhancement of adjuvant functions of Natural Killer T cells using nanovector delivery systems: application in anticancer immune therapy. *Front. Immunol* 8, 879.
- [49] Yuan, W., Qi, X., Tsang, P., Kang, S.J., Illarionov, P.A., Besra, G.S., Gumperz, J., Cresswell, P., 2007. Saposin B is the dominant saposin that facilitates lipid binding to human CD1d molecules". *Proc. Natl. Acad. Sci. U.S.A.* 104, 5551–5556.
- [50] Darmoise, A., Maschmeyer, P., Winau, F., 2010. The immunological functions of saposins. *Adv. Immunol.* 105, 25–62.
- [51] Nakamura, T., Kuroi, M., Harashima, H., 2015. Influence of endosomal escape and degradation of α -galactosylceramide loaded liposomes on CD1d antigen presentation. *Mol. Pharmaceutics* 12, 2791–2799.
- [52] Korsholm, K.S., Agger, E.M., Foged, C., Christensen, D., Dietrich, J., Andersen, C.S., Geisler, C., Andersen, P., 2007. The adjuvant mechanism of cationic dimethyloctadecylammonium liposomes. *Immunology* 121, 216–226.